Redox Biology 18 (2018) 158–172

Contents lists available at ScienceDirect

Redox Biology

journal homepage: www.elsevier.com/locate/redox

Research Paper

Breast cancer susceptibility protein 1 (BRCA1) rescues neurons from cerebral ischemia/reperfusion injury through NRF2-mediated antioxidant pathway

Pengfei Xu[a,1], Qian Liu[a,1], Yi Xie[a], Xiaolei Shi[b,c], Yunzi Li[a], Mengna Peng[a], Hongquan Guo[d], Rui Sun[e], Juanji Li[a], Ye Hong[a], Xinfeng Liu[a,*], Gelin Xu[a,*]

[a] Department of Neurology, Jinling Hospital, Medical School of Nanjing University, Nanjing, Jiangsu 210002, China
[b] Kinsmen Laboratory of Neurological Research, University of British Columbia, Vancouver, British Columbia, Canada
[c] Department of Neurology, The First Affiliated Hospital, Yijishan Hospital of Wannan Medical College, Wuhu, Anhui 241001, China
[d] Department of Neurology, Jinling Hospital, Southern Medical University, Nanjing, Jiangsu 210002, China
[e] Department of Neurology, Jinling Clinical College of Nanjing Medical University, Nanjing, Jiangsu 210002, China

ARTICLE INFO

Keywords:
BRCA1
Ischemia/Reperfusion
Oxidative stress
DNA damage
NRF2

ABSTRACT

Cellular oxidative stress plays a vital role in the pathological process of neural damage in cerebral ischemia/reperfusion (I/R). The breast cancer susceptibility protein 1 (BRCA1), a tumor suppressor, can modulate cellular antioxidant response and DNA repair. Yet the role of BRCA1 in cerebral I/R injury has not been explored. In this study, we observed that BRCA1 was mainly expressed in neurons and was up-regulated in response to I/R insult. Overexpression of BRCA1 attenuated reactive oxygen species production and lipid peroxidation. Enhanced BRCA1 expression promoted DNA double strand break repair through non-homologous end joining pathway. These effects consequently led to neuronal cell survival and neurological recovery. Mechanically, BRCA1 can interact with the nuclear factor (erythroid-derived 2)-like 2 (NRF2) through BRCA1 C-terminal (BRCT) domain. The cross-talk between BRCT and NRF2 activated the NRF2/Antioxidant Response Element signaling pathway and thus protected injured neurons during cerebral I/R. In conclusion, enhanced BRCA1 after cerebral I/R injury may attenuate or prevent neural damage from I/R via NRF2-mediated antioxidant pathway. The finding may provide a potential therapeutic target against ischemic stroke.

1. Introduction

Ischemic stroke, with a sudden reduction of cerebral flow, induces neuronal damage and neurological dysfunction, which may further deteriorate after recanalization treatment [1,2]. Reactive oxygen species (ROS)-related oxidative damage has been recognized as the vital pathogenesis of neuronal loss and subsequent memory impairment following brain ischemia/reperfusion (I/R) injury [3–5]. Redox disruption has been associated with deteriorating clinical outcomes in acute ischemic stroke patients [6,7], but the underlying mechanisms remain largely unclear. The uncertainty in the mechanisms involved in cerebral I/R oxidative injury may be responsible for the ineffectiveness of current neuroprotective treatments. Therefore, a better understanding of pathological processes in I/R oxidative attack may provide a clue for establishing therapeutic targets of ischemic stroke.

Breast cancer susceptibility protein 1 (BRCA1), commonly known as

Abbreviations: ARE, antioxidative response element; AD, Alzheimer disease; ALS, amyotrophic lateral sclerosis; BRCA1, breast cancer susceptibility protein 1; BRCT, BRCA1 C-terminal; BER, base excision repair; CaMKII, calcium/calmodulin-dependent protein kinase II; CNS, central nervous system; CA1, cornu ammonis 1; DSBs, double strand breaks; DCX, doublecortin; GFAP, glial fibrillary acidic protein; GFP, green fluorescent protein; GPX3, glutathione peroxidase 3; GPX4, glutathione peroxidase 4; GCLC, glutamate-cysteine ligase catalytic; GCLM, glutamate-cysteine ligase regulator subunit; HO-1, heme oxygenase 1; HR, homologous recombination; 4-HNE, 4-hydroxynonenol; I/R, ischemia/reperfusion; Iba-1, ionized calcium-binding adapter molecule-1; MCAO, middle cerebral artery occlusion; NRF2, nuclear factor (erythroid-derived 2)-like 2; NQO1, NAD(P)H dehydrogenase (quinone 1); NHEJ, non-homologous end joining; NER, nucleotide excision repair; NPCs, neural precursor cells; NSCs, neural stem cells; 3-NT, 3-nitrotyrosine; 8-OHDG, 8-hydroxy-2′-deoxyguanosine; OGD, oxygen-glucose deprivation; PSD95, postsynaptic density protein 95; ROS, reactive oxygen species; SOD1, superoxide dismutase 1; SOD2, superoxide dismutase 2; XRE, xenobiotic responsive element

* Correspondence to: Department of Neurology, Jinling Hospital, Medical School of Nanjing University, 305 East Zhongshan Road, Nanjing, Jiangsu 210002, China
E-mail addresses: xfliu2@vip.163.com (X. Liu), gelinxu@nju.edu.cn (G. Xu).

[1] These authors contributed equally to this work.

https://doi.org/10.1016/j.redox.2018.06.012
Received 2 June 2018; Received in revised form 27 June 2018; Accepted 30 June 2018
Available online 07 July 2018

a tumor suppressor, is encoded by the breast and ovarian cancer type 1 susceptibility gene [8]. BRCA1 exerts a crucial role in regulating oxidative stress [9]. BRCA1 can modulate intracellular ROS level by interacting with nuclear factor (erythroid-derived 2)-like 2 (NRF2) and promoting gene expression of antioxidant response element (ARE), such as HO-1, NQO1, GPX3 and SOD1 [10,11]. Moreover, BRCA1 can repair ROS-induced DNA double strand breaks (DSBs) [12]. In the central nervous system (CNS), BRCA1 is localized in hippocampus neurons [13]. BRCA1 deficiency has been coincided with increased genomic DNA damage, reduced neurite outgrowth and accelerated cognitive decline [14]. Interestingly, BRCA1 expression has been found to be elevated after I/R injury [15], indicating a potential compensatory effect of BRCA1 in I/R-related oxidative stress. Nevertheless, the role of endogenous BRCA1 in acute brain damage and long-term neurofunctional recovery following cerebral I/R has not been fully elucidated. To this end, in mice with middle cerebral artery occlusion (MCAO), we investigated the cellular expression and distribution pattern of BRCA1, explored the role of BRCA1 in neuronal oxidative stress, and addressed the functional domain of the protein directing the signaling transduction in neuroprotection.

2. Materials and methods

2.1. Lentiviral construction and orthotopic injection

Vector construction was performed by Cyagen Bioscience Inc (Guangzhou, China). To obtain BRCA1-encoding vector (pLV[Exp]-EGFP: T2A: Puro-EF1A-mBrca1), the entire Mus musculus BRCA1 sequence was cloned in pLV/EF1A/EGFP plasmid. The vector pLV[Exp]-EGFP: T2A: Puro-Null was used as control. The virus was packaged using Lenti-XTM HTX packaging system (Clontech, USA). Briefly, HEK-293FT cells were transfected with BRCA1-encoding or control plasmid to produce lentivirus. Lentiviruses were further purified by CsCl gradient centrifugation (30,000 rpm, 4 °C, 16 h) to increase concentration (10^9 TU/mL). The purified lentiviruses were injected into the right lateral ventricle (dosage: 5 μl; coordinates: a/p, +0.4, m/l, +1.0, d/v, –3.5) and hippocampus (dosage: 3 μl; coordinates: a/p, −1.5, m/l, +1.0, d/v, –2.0) of mice using stereotaxic apparatus. The transfection efficiency was measured with GFP immunofluorescence and western blotting. MCAO surgery was performed 14 days after transfection.

2.2. Focal cerebral ischemia

Adult male C57BL/6 J mice (n = 171, weighting 20–25 g) were purchased from Model Animal Research Institute of the Nanjing University (Nanjing, China) and housed under controlled conditions (humidity 55–60%; temperature 23 ± 2 °C and 12-h-light-dark cycle) with food and water freely available. All experiments were approved by Experimental Animal Ethic Committee of Jinling Hospital and were implemented according to National Institutes of Health Guide for the Care and Use of Laboratory Animals (NIH Publication No. 80–23, revised in 1996). Mice were randomized into four groups and received treatments as shown in Fig. S1.

Transient focal cerebral ischemia was induced by intraluminal MCAO surgery following previous method [16]. Briefly, after anesthetized with 2% isoflurane in O_2, the right common carotid artery, internal carotid artery (ICA) and external carotid artery (ECA) were carefully separated. Then a silicon-coated monofilament (diameter 0.16 mm) was inserted into ECA and advanced into ICA until mild resistance was felt. A decline of regional cerebral blood flow (rCBF) > 75% was considered successful interrupt of MCA blood flow monitored by a laser doppler flowmetry (PeriFlux 5010; Perimed AB, Sweden). After 90 min of occlusion, the monofilament was withdrawn for reperfusion. A heating pad was used to maintain the body temperature during surgery. The sham-operated mice underwent the same procedures except that the MCA was not occluded after the neck incision.

2.3. Cerebral infarct volume and brain edema determination

The 2, 3, 5-triphenyltetrazoliumchloride (TTC, Sigma, USA) staining was performed 24 h after reperfusion to measure infarct volume. The 1-mm-thick brain slices were stained with 2% TTC solution at 37 °C for 15 min in dark, followed by overnight fixing with 4% paraformaldehyde (PFA) at 4 °C. The stained slices were scanned using HP Scanjet G3110, and the infarct volume and edema ratio were analyzed with Image-Pro Plus 6.0 software (Media Cybernetics, USA) as reported by others [16]. Briefly, the relative infarct volume (%) was calculated as: (contralateral hemisphere volume − undamaged volume in ipsilateral hemisphere)/(contralateral hemisphere volume × 2)*100%, the relative edema volume (%) was calculated as: (ipsilateral hemisphere volume − contralateral hemisphere volume)/(contralateral hemisphere volume × 2)*100%.

2.4. Neurological deficit evaluation and behavioral analysis

The modified neurologic severity score (mNSS) was used to assess neurological deficits 24 h after reperfusion as described by Chen et al. [17]. The scoring system contains three tests including motor test, sensory test and beam balance test, in which 0 represents no deficit and 14 represents maximal deficits.

Open field test (OFT) was performed to evaluate spontaneous activity and adaptability for 10 mice of each group at day 21 after MCAO surgery using a computerized tracking system (Noldus EthoVision XT, shanghai, China). The animals were placed individually in the corner of an open square (50 cm × 50 cm × 40 cm) in a quiet environment, the total distance traveled, the rearing activities, the time spent and the frequency of entry into the central area (30 × 30 cm^2) were automatically recorded by a digital camera on the top of the square for 30 min per mouse.

Spatial learning and memory were evaluated at day 22–28 after surgery by Morris Water Maze (MWM) test [18]. Firstly, the mice were trained to find the escape platform with cues. Then the mice were trained to find the platform in four trials per day for 5 consecutive days (n = 10 mice per group). If mice failed to reach the platform within 60 s, they would be manually guided to the platform and remained there for 10 s before being placed back to cage. At last, the platform was removed to perform probe trial, and each subject was allowed to search the platform for 60 s. The escape latency to find the platform, the swim path length, the time spent in the target quadrant and platform crossovers were tracked and analyzed by the ANY-maze video tracking software (Stoelting, USA).

2.5. Histological staining and MDA assay

Mice were deeply anesthetized with chloralhydrate (120 mg/kg, i.p.) and intracardially perfused with phosphate-buffered saline (PBS) followed by 4% PFA. Brains were then embedded in optimal cutting temperature compound (Sakura Finetek, USA) and cut coronally into 15 μm or 25 μm sections. Brain sections or neuronal coverslips were fixed with 4% PFA for 20 min before immunostaining. The levels of MDA were detected by Lipid Peroxidation MDA Assay Kit (Beyotime, China).

2.6. Immunofluorescence and TUNEL staining

Sections were blocked in a solution containing 5% goat serum, 1% BSA and 0.3% Triton X-100 for 1 h. The slices or coverslips were incubated with primary antibodies overnight against BRCA1 (1:200, Abcam, UK), NeuN (1:500, Millipore, USA), Iba1 (1:100, Santa Cruz Biotechnology, USA), GFAP (1:500, Abcam, UK), γH2A.X (1:200, Millipore, USA), GFP (1:200, Cell Signaling Technology, USA), 8-OHDG (1:200, Abacm, UK), DCX (1:200, Abcam, UK) and MAP2 (1:200, Cell Signaling Technology, USA). Then the specimens were incubated with

appropriate secondary antibodies and DAPI. As for 3-Nitrotyrosine (3-NT) staining, followed by incubated with primary antibody (1:200, Abcam, UK), samples were subsequently incubated with biotinylated goat anti-mouse IgG and horseradish peroxidase (HRP)-streptavidin reagent for 20 min. Immunoreactivity was detected by DAB. Immunofluorescence images were captured by Olympus BX51 microscope.

Apoptotic neuronal cells in the penumbra area were immunostained with NeuN (1:500, Millipore, USA) and Terminal Deoxynucleotidyl Transferase Dutp Nick End Labeling (TUNEL, Beyotime, China) according to the manufacturer' constructions. TUNEL-AP staining (Millipore, USA) was performed to further confirm the apoptotic cells. The positive labeled cells were calculated by Image J software.

2.7. Oxygen-glucose deprivation and reoxygenation (OGD/R)

Primary cortical neurons were dissected from the cortex of embryonic C57BL/6 J mice (E16) followed by previous method [19]. Briefly, the dissection was digested with 0.125% trypsin for 15 min. The single cell mixture was rinsed with PBS, and collected with DMEM medium containing 10% FBS. After the cell attachment to the flask bottom, the medium was replaced with neurobasal medium containing 2% B27 and 1% glutamax. Medium changing was performed every three days.

Primary microglia and astrocytes were cultured and purified according to previously described methods [20,21]. Briefly, cells were harvested from 1 to 3-day neonatal C57BL/6 J mice and cultured in DMEM/F12 containing 10% FBS and 1% penicillin-streptomycin to establish a mixed glia culture system. After being cultured for 10–14 days, microglia cells were collected by shaking (300 rpm for 4–6 h at 37 °C). The remaining attached cells in the flasks were incubated for 24–48 h before astrocyte harvest. Prior to OGD induction, culture medium was replaced with glucose-free DMEM media. Then cells were incubated in an anaerobic chamber equipped with AnaeroPack-Anaero (MGC, Japan) at 37 °C. After 2 or 6 h, cells were returned to normal incubator with normal medium for reoxygenation.

2.8. In vitro lentivirus transfection and cell viability assay

Neurons were infected with lentivirus-BRCA1 (LV-BRCA1) or lentivirus-GFP (LV-GFP) at 5 days in vitro for 48 h (MOI = 10). Positive ratio of GFP fluorescence and variation of BRCA1 expression were detected for transfection efficiency. After transfection, cells of different group were insulted with OGD. Cell viability at 24 h post-OGD was detected with Cell Counting Kit-8 (CCK-8; Dojindo, Japan). Cell death was detected with Propidium Iodide (PI)/Hoechst 33342 assay Kit (Thermofisher, USA).

2.9. DNA tail comet assay and dihydroethidium staining

The comet assay was performed by DNA damage detection Kit (keygentec, China). Briefly, primary neurons were suspended into single cell suspension, followed by single-cell gel electrophoresis. Finally DNA was staining with PI. The comet assay software project (CASP) was used to analyze the DNA tail of comet assay images. The average tail moment of ten fields was recorded and analyzed. For dihydroethidium (DHE) staining, neurons were pre-treated with neurobasal containing DHE (1 μM; Sigma, USA) for 30 min at 37 °C 24 h post-OGD.

2.10. Plasmids construction and dual-luciferase reporter assay

Wild type (WT) xenobiotic responsive element (XRE) sequence (5′-AGT GCA GTG GCG TGA TCT AGT GCA GTG GCG TGA TCT TACGCG TGC TAG CCC GGG C-3′) which located in the promoter of NRF2 and mutant (MUT) XRE sequence (5′-AGT GCAGTG GCG GTA TCT AGT GCA GTG GCG GTA TCT TAC GCG TGC TAGCCC GGG C-3′) were cloned and inserted in the pGL3 control vector to obtain pGL3-NRF2 WT XRE reporter plasmids and pGL3-NRF2 MUT XRE reporter plasmids as previous described [22]. The reporter plasmids and BRCA1 plasmid (pc-BRCA1) or control plasmid (pc-DNA) were co-transfected into HEK-293T cells for 24 h using lipofectamine 3000. Luciferase activity was measured by Dual-Luciferase® Reporter Assay system (Promega, USA) and the results were normalized by endogenous renilla luciferase activity.

Table 1
Primer sequences for real-time PCR.

Primer	Sense primer (5–3′)	Antisense primer (3–5′)
BRCA1	AGTAGCCAGCACCAAACA	AAACCTCACATTCACATCAAA
TNF-α	AGACAGAGGCAACCTGACCAC	GCACCACCATCAAGGACTCAA
IL-6	GCACTAGGTTTGCCGAGTAGA	AAGCTGGAGTCACAGAAGGAG
NRF2	GTCTTTTGTGAATGGGGCTTTT	CAGTGCTCCTATGCGTGAATC
HO-1	CCACATTGGACAGAGTTCACAG	CCTCACAGATGGCGTCACTTC
NQO1	TGGCGTAGTTGAATGATGTCTT	TTCGGTATTACGATCCTCCCT
GPX4	ACGCAGCCGTTCTTATCAATG	GGCAGGAGCCAGGAAGTAATC
GCLC	CATCGGGTGTCCACATCAACT	ATCAATGGGAAGGAAGGGGTAT
GCLM	GCAGAATGTAGCCTTTAGACTTGA	GTGATGCCACCAGATTTGACT
SOD1	ACCGTCCTTTCCAGCAGTCAC	ATGGGTTCCACGTCCATCAGT
SOD2	AGCAGGCAGCAATCTGTAAGC	CACTGAAGTTCAATGGTGGGG
GAPDH	AAGAAGGTGGTGAAGCAGG	GAAGGTGGAAGAGTGGGAGT

2.11. Real-time quantitative PCR analysis

Total RNA was extracted using TRI Reagent (Sigma, USA) and was reverse transcribed into cDNA using RevertAid First Strand cDNA Synthesis Kit (Thermo Scientific, USA). Real-time quantitative PCR was performed in a 25 μl reaction system containing diluted cDNA, specific primers (10 μM) and UltraSYBR Mixture (CWBio, China) using Stratagene Mx3000P QPCR system (Agilent Technologies, USA). The levels of mRNA expression were normalized to the endogenous control GAPDH. The results were expressed as fold changes compared with the control group which was set to 100%. The primer pairs were listed in Table 1.

2.12. Co-immunoprecipitation and GST pull-down assay

Total cell lysates from cortical ischemic penumbra were harvested using weak RIPA lysis buffer (Cell Signaling technology, USA), and were pre-cleared with 50% protein A/G agarose for 1 h. Then 500 μl of extracted proteins were incubated with 2 μg primary antibody or control IgG overnight at 4 °C. The immune complexes were pulled down with protein A/G agarose for 4 h in a 4 °C shaker. Microbeads were collected and washed, and then proteins were eluted through boiling in 2 × loading buffer followed by immunoblotting analysis.

For GST pull-down assay, GST-BRCA1, including GST-BRCA1-1 (aa 15–172), GST-BRCA1–2 (aa 342–503) and GST-BRCA1–3 (aa 1591–1784) were constructed using pGEX-GST vectors and expressed in *E.coli* Rosetta cells. The obtained GST fusion proteins were further purified using glutathione-Sepharose 4B beads. The lysates from cerebral ischemic penumbra were added into the mixture of GST fusion proteins and beads, and incubated for 4 h at 4 °C with shaking. The eluted proteins were analyzed by western blotting.

2.13. Western blotting

Total proteins were prepared using RIPA Lysis Buffer (Cell Signaling technology, USA). Nuclear and cytoplasmic protein were separately extracted using NE-PER Nuclear and Cytoplasmic Extraction Reagents (Thermofisher, USA). Protein concentrations were quantified by BCA Protein Assay Kit (Generay Biotechnology, China). Proteins (15 μg per cell sample and 30 μg per mouse sample) were separated by SDS-PAGE

electrophoresis and then transferred to polyvinylidene difluoride membranes (Millipore, USA). Membranes were blocked with 3% bovine serum albumin and 5% fat-free milk at room temperature for 1.5 h. Then membranes were incubated with primary antibodies against BRCA1 (1:1000, Abcam, UK), p53 (1:1000, Abcam, UK), Bcl-2 (1:1000, Abcam, UK), Bax (1:1000, Cell Signaling technology, USA), Cleaved Caspase-3 (1:1000, Cell Signaling technology, USA), γH2A.X (1:1000, Millipore, USA), RAD51 (1:5000, Millipore, USA), Ku70/80 (1:1000, Abcam, UK), pDNA-PKcs (1:1000, Abcam, UK), DNA-PKcs (1:1000, Abcam, UK), NRF2 (1:1000, Abcam, UK), NQO1 (1:1000, Abcam, UK), HO-1 (1:200, Santa Cruz, USA), GPX4 (1:1000, Abcam, UK), PSD95 (1:1000, Abcam, UK), CaMKII (1:1000, Abcam, UK), Synapsin I (1:200, Santa Cruz, USA), Synaptophysin (1:1000, Abcam, UK), GST (1:50000, Cell Signaling technology, USA), histone H3 (1:3000, Cell Signaling technology, USA) and β-actin (1:4000, Cell Signaling technology, USA) overnight at 4 °C, followed by incubated with HRP-conjugated secondary antibody at room temperature. Protein signals were detected by enhanced chemiluminescence (Millipore, USA) and were analyzed by Image J software.

2.14. Statistical analysis

Statistical analyses were performed using SPSS 22.0 software (SPSS Inc., IBM, NY, USA). Path length and escape latency data in MWM test were analyzed by repeated-measures analysis of variance (ANOVA) followed by least-significant difference (LSD) post hoc test. The neurological scores were analyzed using the Kruskal-Wallis test followed by Dunn post hoc test. Other results were analyzed by independent sample *t*-test (for two groups) and one-way ANOVA followed by LSD post hoc test (for multiple groups). Data are presented as median (range) for mNSS assessment and mean ± SD for other experiments. $P < 0.05$ was considered of statistical significance.

3. Results

3.1. BRCA1 was triggered by cerebral ischemic stroke in vivo and vitro

Immunostaining demonstrated that BRCA1 signals were observed primarily in the ipsilateral cortex, but not in the striatum and hippocampus (Fig. 1**A**). BRCA1 expression was mainly detected in cytoplasm and nuclei of the NeuN positive neurons, but not in the Iba1 positive microglia or GFAP positive astrocytes in the peri-infarct region (Fig. 1**A**, **B**). Additionally, in brain cortex of sham-operated mice, BRCA1 immunofluorescence intensity was weak and mainly expressed in cytoplasm of neuronal cells (Fig. S2). These results suggested that BRCA1 signal was induced and expressed in ischemia involved neurons. The consistent induction on BRCA1 was also detected in OGD injured neuron in vitro (Fig. 1**C**, $P = 0.009$). However, expression or up-regulation of BRCA1 by OGD injury was rarely detected in cultured astrocyte and microglia (Fig. 1**C**). Immunofluorescence results further corroborated that BRCA1 was well co-localized with MAP2, a marker of primary neurons (Fig. 1**D**). Similar to the observation in vivo, BRCA1 was mainly localized to the cytoplasm of primary neurons under normal condition, and significantly increased in cytoplasm and nucleus after OGD challenge (Fig. 1**D**).

Western blotting analysis indicated that BRCA1 gradually increased from the 2nd hour and reached a plateau at day 1 after reperfusion in ischemic penumbra, thereafter declined toward the baseline level (Fig. 1**E**). Meanwhile, the expression of BRCA1 in the ischemic core was sharply enhanced at the 2nd hour after reperfusion (Fig. 1**F**). Furthermore, the expression of BRCA1 was induced by OGD in a time-depend manner, and back to the baseline level at the 6th hour after reoxygenation (Fig. 1**G**). The same mRNA expression pattern of BRCA1 was detected through real-time PCR analysis both in vivo and vitro (Fig. S3**A**, **B**).

3.2. BRCA1 attenuated neurological deficits following ischemic stroke

To explore the role of BRCA1 in ischemic stroke, LV-BRCA1 or LV-GFP (for GFP fluorescence control) was injected into the right lateral ventricle and hippocampus of mice. BRCA1 displayed a 4.91-fold higher expression following LV-BRCA1 transfection (Fig. 2**A**, **B**, $P < 0.001$). Real-time quantitive PCR detected that inflammatory gene expressions of IL-6 and TNF-α were not significantly influenced by the lentivirus injection (Fig. 2**C**). These data suggested that the lentivirus was effective and did not induce significant inflammatory response.

TTC staining results revealed that LV-BRCA1 administration significantly reduced infarct volume (by 27.8%) and brain edema (by 43.1%) compared to MCAO mice (Fig. 2**D-F**, $P = 0.002$ and $P < 0.001$ respectively). The consistently attenuated neurological deficits with LV-BRCA1 transfection was evaluated by mNSS assessment (Fig. 2**G**, $P = 0.009$).

3.3. BRCA1 improved long-term neurobehavioral function

OFT at day 21 after reperfusion revealed that the spontaneous locomotion in the center, the total locomotion, the rearing activities, the spent time and the frequency of entry into the central area were significantly reduced in MCAO group than that in sham group; whilst transfection with LV-BRCA1 significantly abolished these reductions **(**Fig. 3**A–E)**.

Cognitive function was assessed by MWM. According to the LSD post hoc analysis, all experimental mice benefited from the 5-day acquisition of spatial training, MCAO mice swam longer distance and spent longer time to find the platform than sham mice; whilst the LV-BRCA1 transfection notably attenuated this spatial learning deficit on the 4th and 5th day of training (Fig. 3**F–H**, for path length: $P = 0.046$ and 0.011 respectively; for escape latency: $P = 0.004$ and 0.010 respectively). In the probe phase, LV-BRCA1 transfection abolished the MCAO-induced reduction on the crossovers of platform location and the percentage of time spent in target quadrant ($P = 0.041$ and 0.011 respectively), while there were no statistical differences between MCAO and LV-GFP mice (Fig. 3**F, I, and J**). These tests indicated a potential protective effect of BRCA1 on the long-term neurobehavioral recovery following ischemic stroke.

3.4. BRCA1 overexpression alleviated ischemia/reperfusion induced neuronal apoptosis

As neuronal apoptosis is a major cause of neurological dysfunction, we set out to detect the role of BRCA1 in neuronal apoptosis. TUNEL/NeuN and TUNEL-AP staining results manifested that LV-BRCA1 treatment can mitigate neuronal apoptosis in the peri-infarct region 1 day after reperfusion (Fig. 4**A, B**, $p = 0.001$).

Given that BRCA1 deficit can induce p53-dependent proapoptotic pathways in early neural progenitors [23], we investigated the relative signaling proteins to probe the role of BRCA1 in neuronal apoptotic cascades following I/R injury. Protein levels of p53, Bax and Cleaved Caspase-3 were all markedly increased 1 day after MCAO, but these increments were significantly attenuated by LV-BRCA1 administration (Fig. 4**C**, $P = 0.021$, 0.001 and 0.009 respectively). In addition, LV-BRCA1 administration significantly reversed the decreased expression of Bcl-2, an anti-apoptotic protein, in MCAO mice (Fig. 4**C**, $P = 0.038$). These data indicated a potential role of BRCA1 in monitoring the dynamic equilibrium of apoptosis genes, therefore protects neurons against I/R-induced apoptosis.

To further confirm the role of BRCA1 in neuronal ischemic injury, primary cultured cortical neurons were transfected with LV-BRCA1 (Fig. S4**A**). Western blotting detected a 4.40-fold up-regulation of BRCA1 after LV-BRCA1 transfection (Fig. S4**B**, $P < 0.001$). As manifested in Fig. S4**C-E**, OGD/R administration significantly induced neuronal death, whilst overexpression of BRCA1 remarkably reduced the

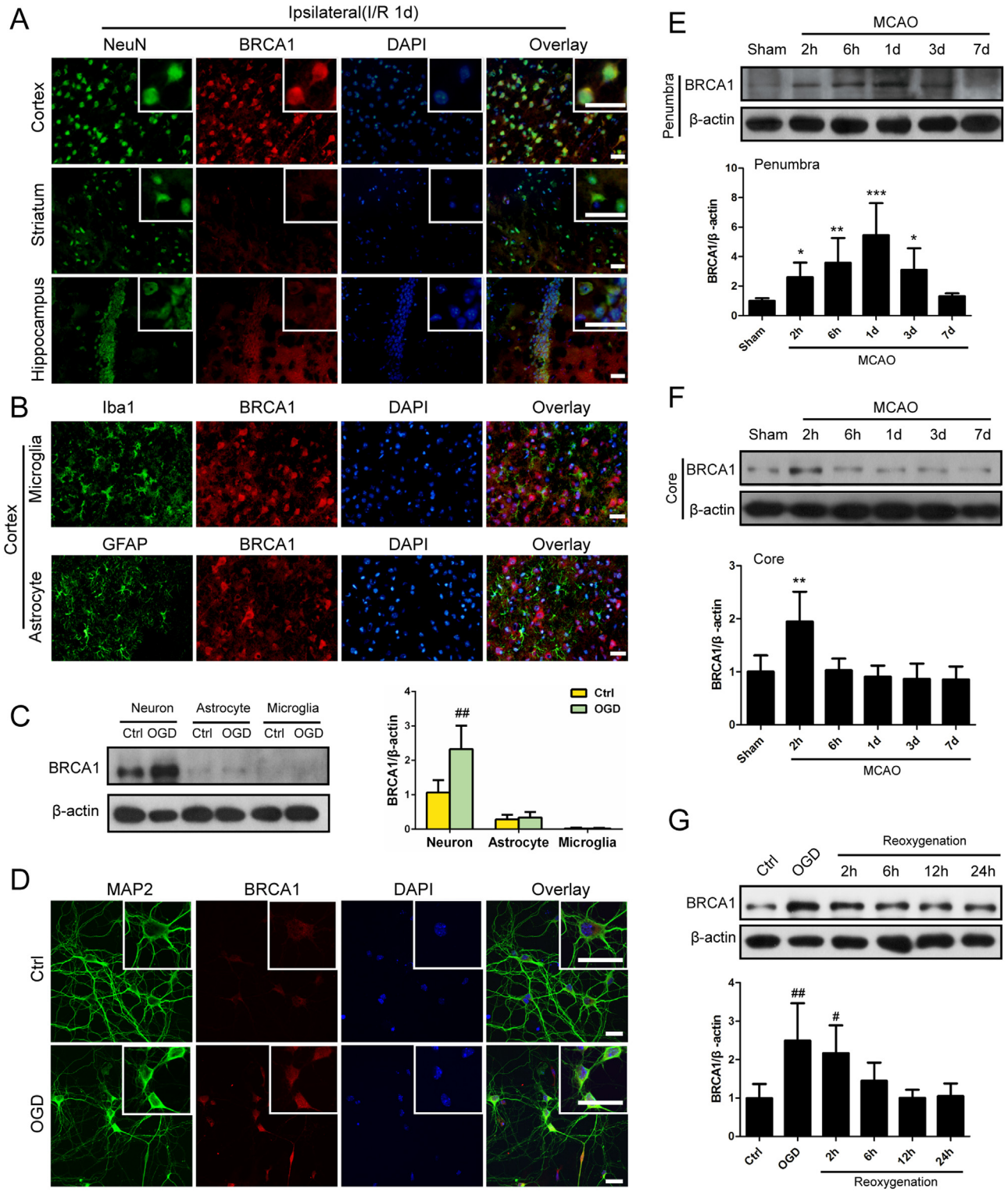

Fig. 1. BRCA1 was up-regulated in neurons following ischemic stroke. (A, B) Double immunostaining of BRCA1 with Iba-1 (microglia marker), GFAP (astrocyte marker) and NeuN (neuron marker) were performed in mice brain sections 1 day after reperfusion. Insets show a higher magnification view. Scale bar = 20 μm. (C) Immunoblots and quantitative analysis of BRCA1 in cultured neurons, astrocytes and microglia. (D) Representative immunofluorescence images of BRCA1 co-stained with MAP2 in control and OGD neurons. Insets show a higher magnification view. Scale bar = 20 μm. (E, F) The protein expression pattern and time course of BRCA1 in ischemic penumbra and ischemic core. (D) Immunoblots of BRCA1 in OGD-treated neurons and quantification. All results are presented as mean ± SD; n = 6 for all groups; $^{*}P < 0.05$, $^{**}P < 0.01$, $^{***}P < 0.001$ versus sham mice; $^{\#}P < 0.05$, $^{\#\#}P < 0.01$ versus control mice.

neuronal damage ($P = 0.001$ and 0.002 respectively). No significant differences on cell death and cell viability between OGD/R and LV-GFP groups were detected, which excluded the possibility of overt cellular toxicity from the recombinant lentivirus transfection. These results also indicated a critical role of BRCA1 in monitoring I/R-induced neuronal apoptosis.

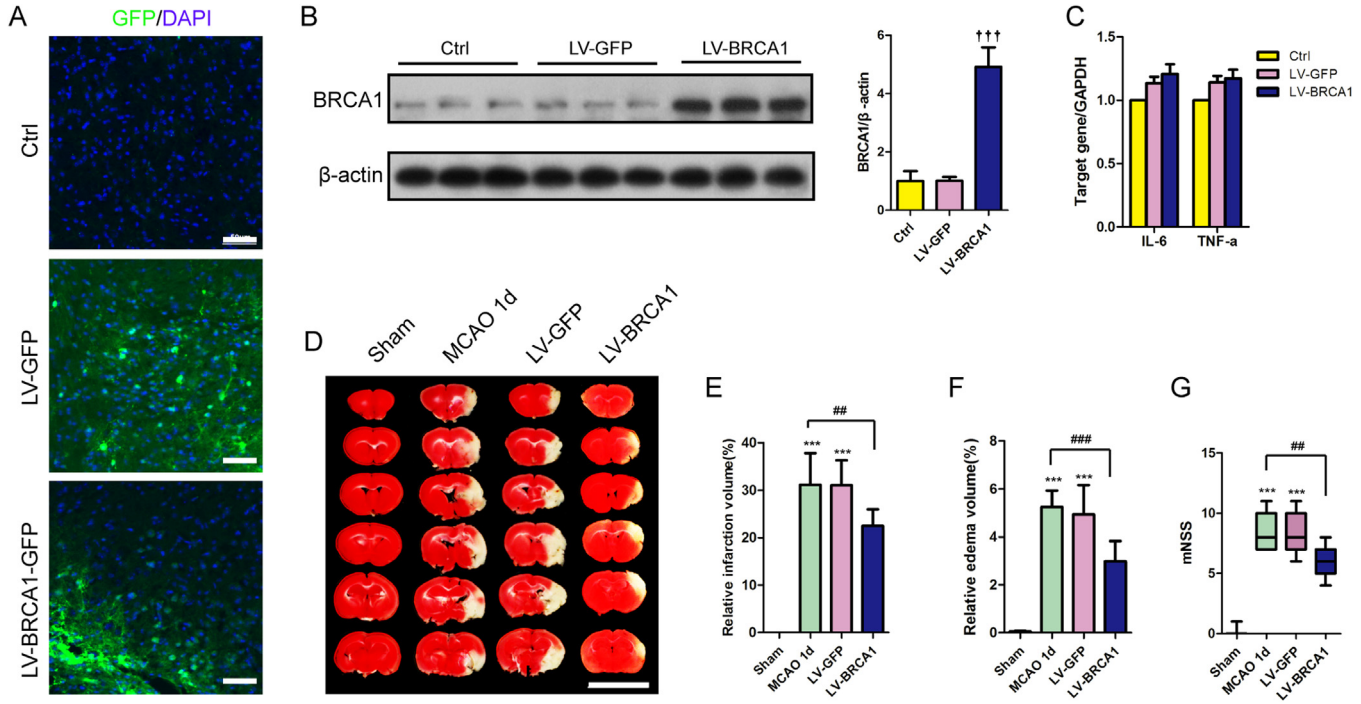

Fig. 2. BRCA1 up-regulation attenuated brain I/R injury. LV-GFP or LV-BRCA1 was injected into the right lateral ventricle and right hippocampus of mice 14 days before MCAO surgery. (A) Brain sections were immunostained for GFP (green) and DAPI (blue). Scale bars = 50 μm. (B) Immunoanalysis and quantification of BRCA1, n = 5. (C) Quantitative real-time PCR analysis of IL-6 and TNF-α, n = 5. (D) Representative image of TTC staining in the indicated groups 1 day after reperfusion. Scale bar = 1 cm. (E, F) Quantitative analysis of infarct volume and edema volume, n = 9. (G) Neurological scores assessment, n = 20. Data are shown as median (range) for neurological scores and mean ± SD for others; $^{\dagger\dagger\dagger}P < 0.001$ versus control mice; $^{***}P < 0.001$ versus sham mice; $^{\#\#}P < 0.01$, $^{\#\#\#}P < 0.001$ versus MCAO mice.

3.5. BRCA1 reduced neuronal DNA damage induced by I/R injury

Given the pivotal role of BRCA1 in repair of DSBs [24], we investigated the role of BRCA1 in neuronal DSBs damage induced by I/R injury. We immunostained the brain sections with antibody targeting on γH2A.X for evaluating DNA damage [25]. As depicted in Fig. 5**A** and **B**, a robust increment of γH2A.X positive foci was observed in peri-infarct region of MCAO mice, which was remarkably abolished by LV-BRCA1 transfection ($P < 0.001$). Meanwhile, LV-BRCA1 transfection lead to a 57.4% decrease in γH2A.X expression (Fig. 5**C**, $P = 0.038$). We next analyzed the effect of LV-BRCA1 treatment on the expressions of molecules in homologous recombination (HR) and non-homologous end joining (NHEJ) repair pathway. RAD51 was utilized to evaluated HR repair pathway, while Ku80, Ku70 and pDNA-PKcs were used to evaluate NHEJ repair pathway. Immunoblotting results showed that I/R injury significantly increased the levels of RAD51, Ku80, Ku70 and the ratio of pDNA-PKcs (Thr2609)/DNA-PKcs comparing to the sham group (Fig. 5**C, D**); whilst LV-BRCA1 treatment further strengthened the levels of Ku70 and Ku80 (Fig. 5**C**, both $P < 0.001$). However, no significant changes in RAD51 level and pDNA-PKcs (Thr2609)/DNA-PKcs ratio were observed between MCAO group and LV-BRCA1 group (Fig. 5**C, D**).

Moreover, we found that OGD/R-induced violent DNA damage was markedly suppressed by LV-BRCA1 (Fig. S5**A, B**, $P = 0.041$). LV-BRCA1 administration markedly reduced γH2A.X level and strengthened Ku70 and Ku80 expression in OGD/R neurons (Fig. S5**C**, $P = 0.016$, 0.004 and $P < 0.001$ respectively). However, no significant difference concerning RAD51 expression was detected between LV-BRCA1 and OGD/R groups (Fig. S5**C**). These observations corroborated with results observed in vivo. Taken together, these results suggested that BRCA1 may promote neuronal DSBs repair after focal cerebral I/R injury via NHEJ repair pathway.

3.6. BRCA1 overexpression protected neurons against oxidative injury

Although BRCA1 has not been directly linked to neural oxidative stress, it has been reported to down-regulate ROS production in human breast carcinoma cell lines [11]. This study investigated the role of BRCA1 in neuronal oxidative stress induced by MCAO. As shown in Fig. 6**A–C**, I/R injury significantly increased the number of 8-OHDG positive cells by 38.0-fold and 3-NT positive cells by 24.8-fold in peri-infarct region; whilst the increments were largely avoided after LV-BRCA1 transfection ($P = 0.040$ and 0.011 respectively). ROS production and antioxidative enzyme level were also analyzed. As shown in Fig. 6**D and E**, comparing with sham mice, MCAO or LV-GFP mice were detected with higher ROS and lower SOD enzyme productions; whilst the increment of ROS and decrease of SOD were both reversed in LV-BRCA1 transfected mice ($P = 0.007$ and 0.036 respectively). We then examined the effect of BRCA1 overexpression on lipid peroxidation, which is another type of oxidative damage. I/R injury significantly augmented the MDA level and the 4-HNE protein adducts in ischemic cortex, while LV-BRCA1 transfection attenuated these increments (Fig. 6**F, G** $P = 0.006$ and 0.041 respectively).

To examine whether BRCA1 is involved in ROS production in primary neurons, DHE staining was performed to evaluate the intracellular ROS level. LV-BRCA1 transfected group displayed a 29.5% reduction of DHE positive cells compared with non-infected group (OGD/R group) 3 h after OGD, whilst LV-GFP administration had no effect on ROS production (Fig. S5**D, E**, $P = 0.016$ and 0.999 respectively). Overall, these results indicated the antioxidative effect of BRCA1 in preventing neuron damage from I/R.

3.7. BRCA1 triggered NRF2/ARE signaling pathway

Because BRCA1 regulates NRF2 expression [9,10], we focused on NRF2 to further investigate BRCA1-involved neuronal antioxidation

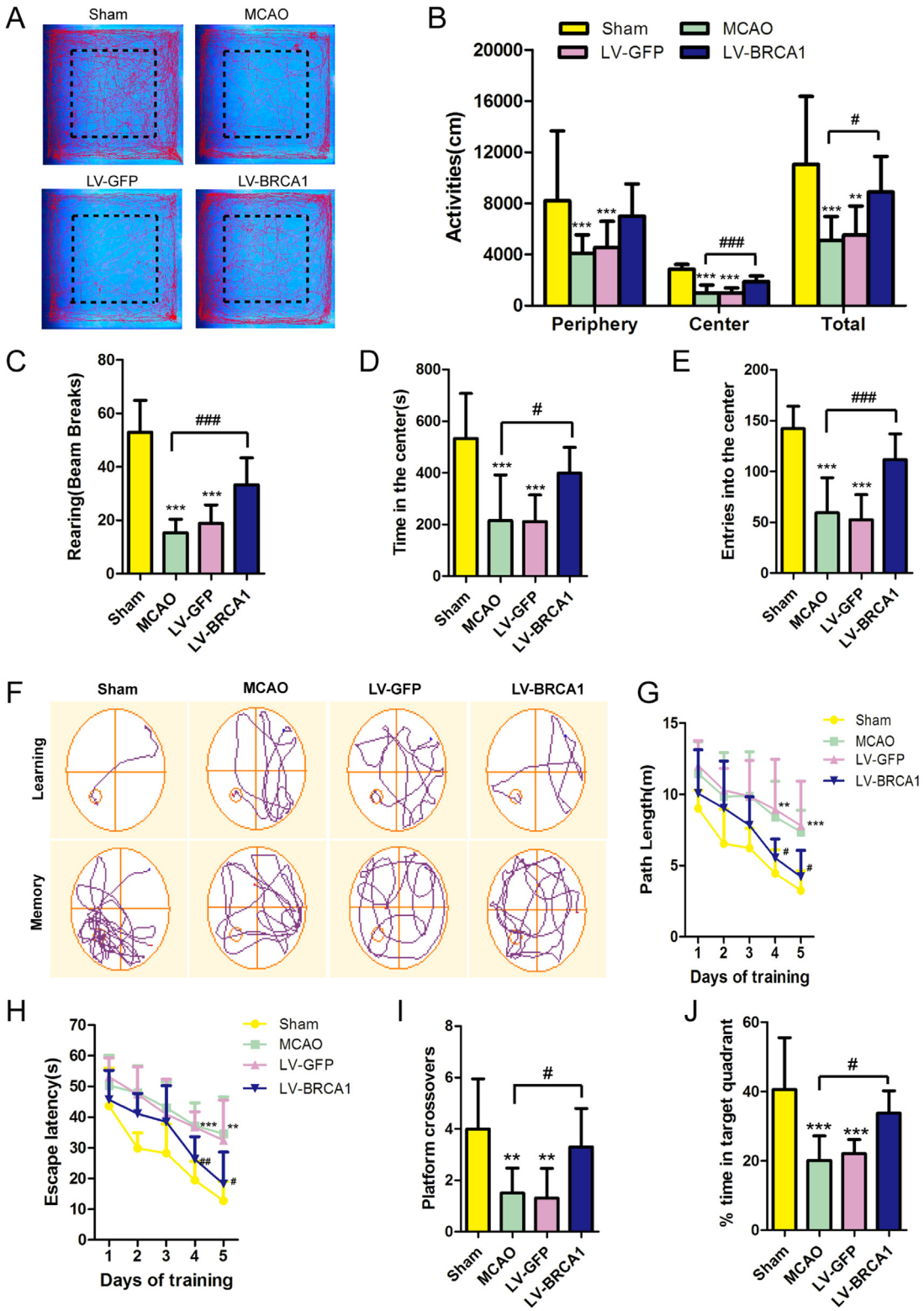

Fig. 3. Administration of LV-BRCA1 rescued I/R-induced cognitive deficits. (A) Representative tracks of movements of mice for 30 min in an open field box. (B) Cumulative distance traveled per zone. (C-E) Total rearing activities, the time spent in and the frequency entry into the center area during the 30 min session in the OFT. (F) Representative swim path traces of mice in hidden platform test (top traces, "learning") and probe phase (bottom traces, "memory"). (G) The swim path and (H) escape latency were recorded at day 23–27 after MCAO. (I) Platform crossovers and (J) the percentage of time spent in the target quadrant were recorded at day 28 after MCAO in probe trails. Data are shown as mean ± SD; n = 10 for all groups; $^{**}P < 0.01$, $^{***}P < 0.001$ versus sham mice; $^{\#}P < 0.05$, $^{\#\#}P < 0.01$, $^{\#\#\#}P < 0.001$ versus MCAO mice.

after cerebral I/R injury. Co-immunoprecipitation assay indicated an interaction between BRCA1 and NRF2 (Fig. 7**A**). BRCA1 possesses varies of functional domains which can combine with different signaling proteins [8]. To determine the binding domain of BRCA1 to NRF2, three GST-tagged BRCA1 domains (aa 15–172, aa 342–503 and aa 1591–1784, Fig. 7**B**) were synthesized, purified and incubated with

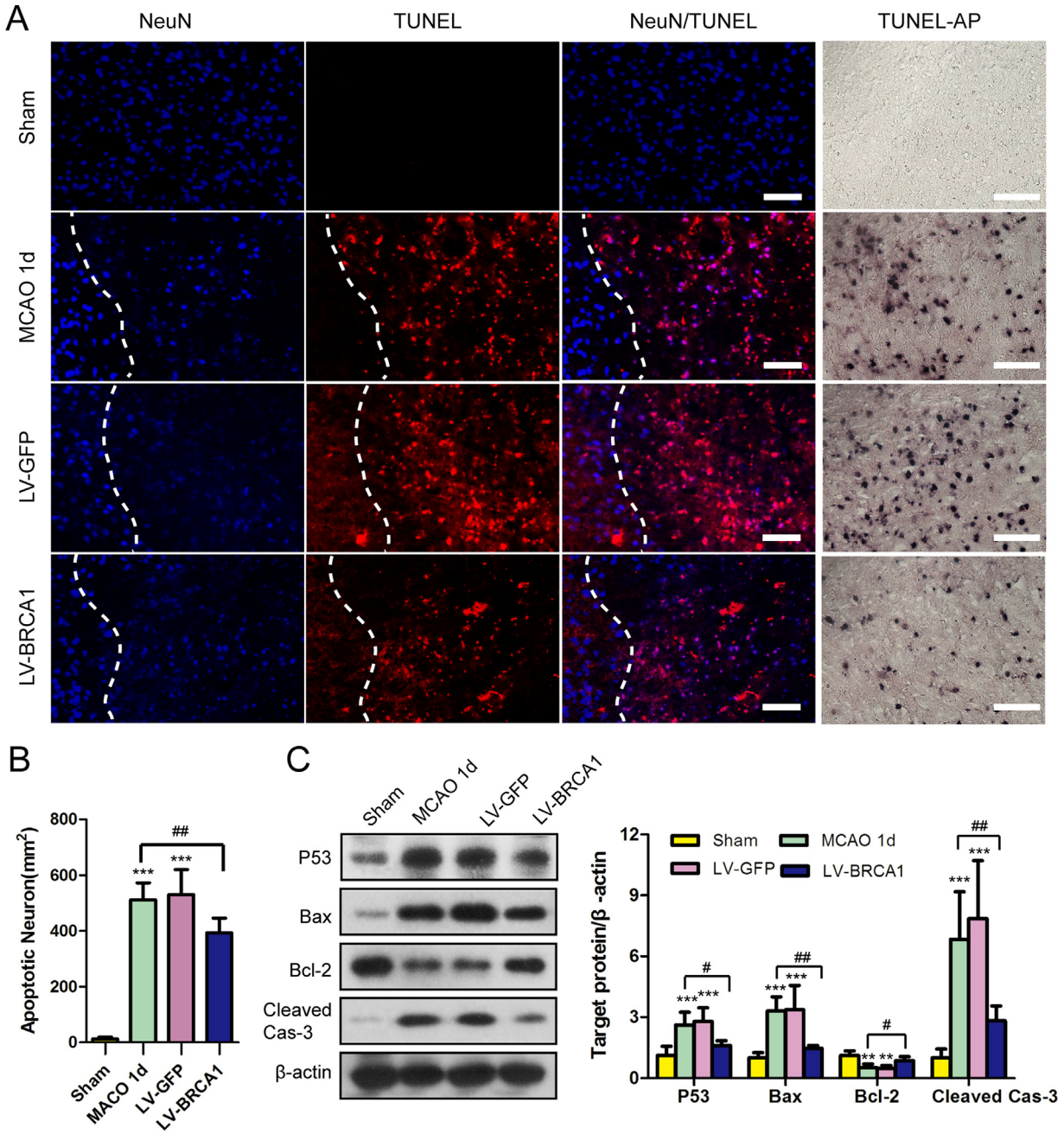

Fig. 4. BRCA1 overexpression ameliorated neuronal apoptosis after I/R. (A) Apoptotic neurons were detected by NeuN/TUNEL and TUNEL-AP staining 1 day after reperfusion. Scale bars = 50 μm. (B) Positive apoptotic neurons were calculated using Image J in nine random fields. (C) Western blot and quantitative analysis of p53-dependent proapoptotic proteins in brain extracts of the indicated groups, including p53, Bax, Bcl-2 and Cleaved Caspase-3. n = 6. Data are expressed as mean ± SD; $^{**}P < 0.01$, $^{***}P < 0.001$ versus sham group; $^{\#}P < 0.05$, $^{\#\#}P < 0.01$ versus MCAO group.

the tissue lysate of cerebral ischemic penumbra. The specific protein-to-protein interaction was detected between BRCT domain (aa 1591–1784) and NRF2 (Fig. 7**B**). Western blotting and real-time PCR analyses demonstrated that LV-BRCA1 transfection significantly enhanced NRF2 expression one day after I/R (Fig. 7**C, D**, $P < 0.001$ and $P = 0.008$ respectively). Besides, LV-BRCA1 transfection significantly up-regulated nuclear NRF2 level (Fig. 7**C**, $P < 0.001$), which suggested that BRCA1 overexpression promoted nuclear translocation of NRF2.

Dual-luciferase report gene assay showed that overexpression of BRCA1 significantly enhanced the WT XRE-containing promoter activity of NRF2 (Fig. 7**E**, $P < 0.001$), whilst no activation was detected in NRF2 reporter containing MUT XRE sequence. The result suggested that BRCA1 can bind to NRF2 promoter, which may influence NRF2 transcription. It has been reported that NRF2 targeting a plenty of genes which contain ARE in their promoter [26]. We then detected ARE genes after LV-BRCA1 treatment. By real-time PCR, LV-BRCA1 substantially enhanced mRNA levels of HO-1, NQO1, GPX4, GCLC and SOD2 in cerebral ischemic penumbra (Fig. 7**F**, $P = 0.011$ for HO-1, $P < 0.001$ for others). While, no significant differences were detected in mRNA levels of GCLM and SOD1 between MCAO and LV-BRCA1 groups (Fig. 7**F**). Moreover, LV-BRCA1 administration noticeable strengthened the protein levels of HO-1, NQO1 and GPX4 in MCAO mice (Fig. 7**G**, $P < 0.001$ for all). Consistently, LV-BRCA1 transfection significantly enhanced the protein levels of NRF2, HO-1 and NQO1 in OGD/R neurons (Fig. S5**F**, $P < 0.001$ for all). Collectively, these results indicated a

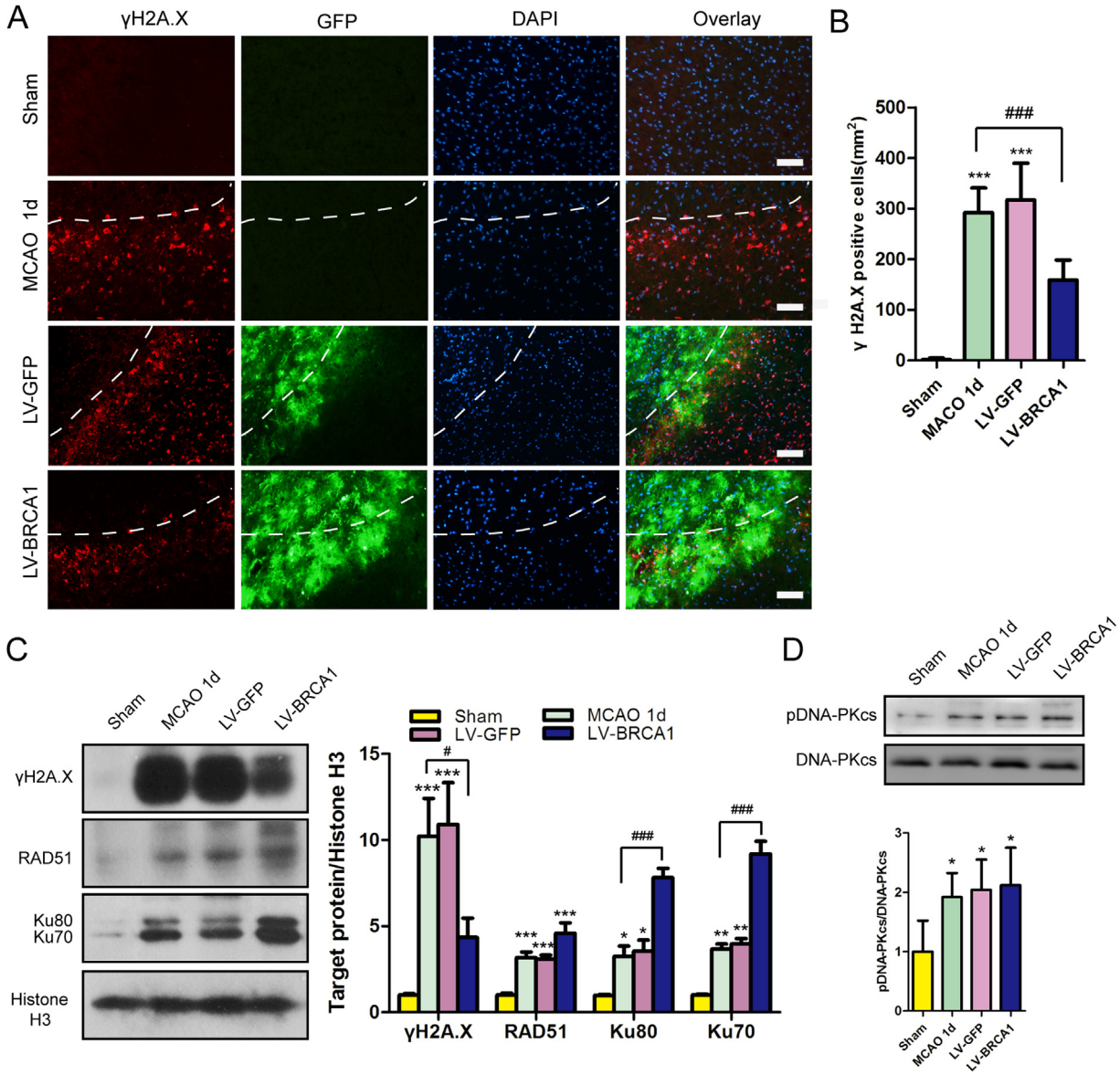

Fig. 5. BRCA1 overexpression reduced DSBs after I/R. (A) Representative photomicrographs of γH2A.X staining. Scale bar = 50 μm. (B) Statistical analysis of γH2A.X positive cells, n = 9 fields from six mice. (C) Western blot analysis and quantification of nuclear γH2A.X, RAD51, Ku80 and Ku70 in cerebral ischemic penumbra cortex, n = 6. (D) Western blot analysis and quantification of nuclear phosphorylation of DNA-PKcs and DNA-PKcs, n = 6. Data are shown as mean ± SD; $^{*}P < 0.05$, $^{**}P < 0.001$, $^{***}P < 0.001$ versus sham group; $^{\#}P < 0.01$, $^{\#\#\#}P < 0.001$ versus MCAO group.

positive regulation of BRCA1 on NRF2/ARE signaling pathway, which may attenuate neuronal oxidative damage.

3.8. BRCA1 promoted synaptic plasticity after ischemic stroke

GFP immunofluorescence and western blotting results indicated that LV-BRCA1 injection markedly enhanced BRCA1 expression in hippocampus after MCAO (Fig. 8**A, B**). BRCA1 has been reported to influence synaptic plasticity [14,27], which is a compensatory mechanism for brain rehabilitation after injury. Therefore, we assessed the expressions of synaptogenesis markers, including PSD95, CaMKII, Synapsin I and Synaptophysin in hippocampus on day 28 post-MCAO. As shown in Fig. 8**C**, there is a remarkable reduction of these synaptogenesis markers ($P < 0.001$ for all); whilst LV-BRCA1 infection significantly attenuated the decrease of these proteins ($P = 0.041$, $P < 0.001$, $P = 0.019$ and $P = 0.019$ respectively). Immunostaining of DCX implied that administration of LV-BRCA1 significantly mitigated the reduction of dendritic spine density in cornu ammonis 1 (CA1) region (Fig. 8**D, E**, $P = 0.018$).

4. Discussion

This study demonstrated that BRCA1 was mainly expressed on neurons in peri-infarct area and was elevated after cerebral I/R injury; manipulation of BRCA1 level through genetic overexpression reduced ROS production, lipid peroxidation and DNA damage, resulting in decreased neuronal apoptosis and cerebral infarction, and improved neurological functions; BRCA1 protected neurons through direct interacting with NRF2 via BRCT domain to activate NRF2/ARE antioxidant pathway and promoting DSBs repair through NHEJ pathway; overexpression of BRCA1 in the hippocampus rescued long-term neurobehavioral outcomes post-stroke (Fig. 9). To our knowledge, this investigation has for the first time exposed the neuroprotective function of BRCA1 in ischemic stroke.

In adult rodent CNS, BRCA1 is detected in nuclear of neurons [28]. Existing reports have documented that in Alzheimer brains, BRCA1 is

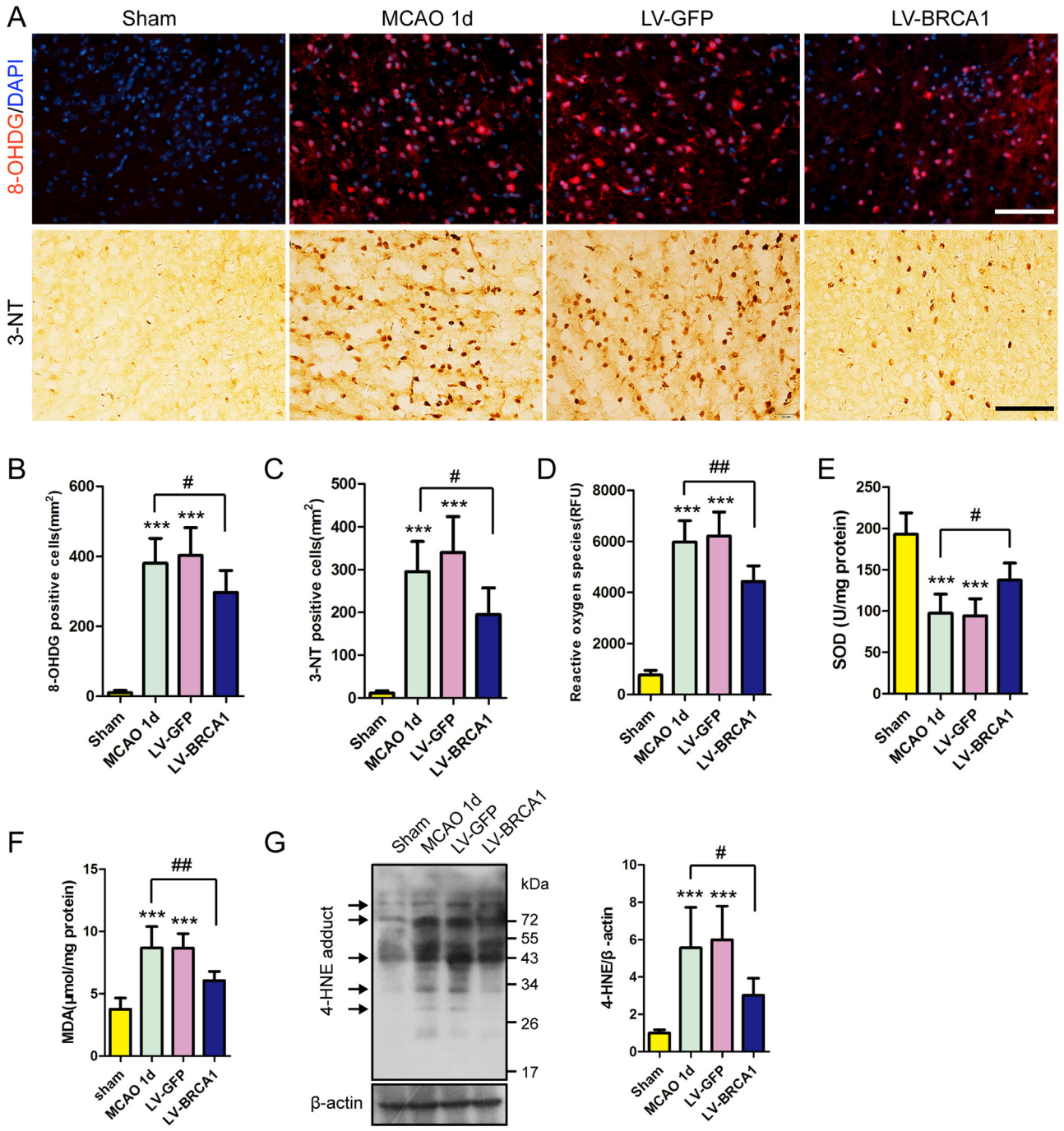

Fig. 6. BRCA1 overexpression attenuated oxidative damage post-stroke. (A) Representative images of 8-OHDG and 3-NT staining and (B, C) statistical analysis, n = 9 fields from six mice. Scale bars = 50 μm. (D) ROS production and (E) SOD enzyme activity assay of the indicated groups, n = 6. Lipid peroxidation was evaluated by MDA assay and western blotting. (F) Histograms showing MDA levels in the four groups, n = 6. (G) Western blot analysis and quantification of 4-HNE protein adducts, n = 6. Arrows indicate bands with changed 4-HNE signal at different protein sizes. Data are shown as mean ± SD; $^{***}P < 0.001$ versus sham group; $^{\#}P < 0.05$, $^{\#\#}P < 0.01$ versus MCAO group.

elevated comparing to clinical normal aged brains and prominent expressed in hippocampal CA1 region and neurofibrillary tangles [13,27,29]. However, there is a conflict report that BRCA1 is reduced in Alzheimer disease (AD) patients and distributed in cytoplasmic and nuclear of hippocampal neurons [14]. In spinal cord of human amyotrophic lateral sclerosis (ALS) patients, BRCA1 is up-regulated and specially expressed in microglia [30]. To date, cellular expression and distribution of BRCA1 in ischemic stroke has yet been clarified, which is the subject of this study. Here, we observed that the BRCA1 was increased and then decreased after I/R injury both in vivo and vitro. Moreover, the up-regulation of BRCA1 was mainly observed in neurons, but not in microglia or astrocytes. The enhanced nuclear expression of BRCA1 signal was observed in neurons after I/R or OGD, suggesting that the nuclear translocation of BRCA1 could be induced by ischemic stress.

Excessive ROS production promotes brain damage post I/R injury through many mechanisms, including brain-blood barrier disruption, inflammation, apoptosis, and cellular necrosis [3]. Inhibiting the production of ROS, removing ROS or repairing oxidative macromolecular damage are the main strategies to combat against oxidative stress

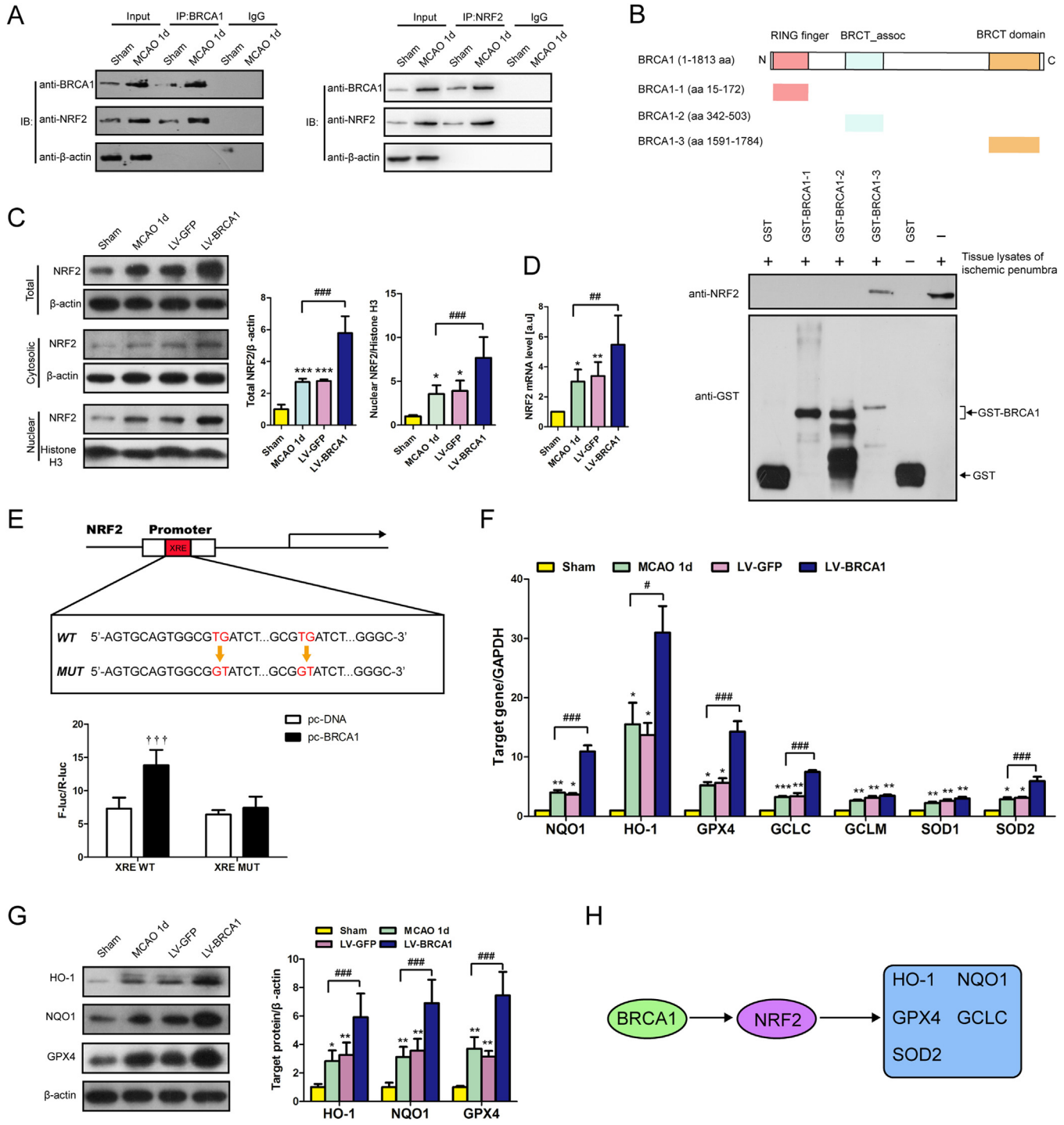

Fig. 7. BRCA1 provoked NRF2-mediated antioxidative pathway. (A) BRCA1 binds to NRF2. The brain lysates were immunoprecipitated with anti-BRCA1 (left) or anti-NRF2 (right) antibodies. Then total lysates and immunoprecipitates were analyzed by immunoblotting with anti-BRCA1 and anti-NRF2. n = 5. (B) Schematic representation of BRCA1 fusion proteins. Interaction was detected between BRCT domians (aa 1591–1784) and NRF2. (C) Western blots showing the protein levels of total, cytosolic and nuclear NRF2, and quantification analysis of total and nuclear NRF2. n = 6. (D) mRNA levels of NRF2 in the indicated groups, n = 6. (E) Dual-luciferase reporter assay of BRCA1 and NRF2 XRE, n = 5. (F) mRNA levels of HO-1, NQO1, GPX4, GCLC, GCLM, SOD1 and SOD2. n = 6. (G) Immunoblots and quantitative analysis of total HO-1, NQO1 and GPX4. n = 6. (H) Schematic diagram of NRF2-mediated antioxidative pathway triggered by BRCA1. Data are expressed as mean ± SD; $^{\dagger\dagger\dagger}P < 0.001$ versus pc-DNA + XRE WT group; $^{*}P < 0.05$, $^{**}P < 0.01$, $^{***}P < 0.001$ versus sham group; $^{\#}P < 0.05$, $^{\#\#}P < 0.01$, $^{\#\#\#}P < 0.001$ versus MCAO group.

damage [2]. Studies have always focused the antioxidant effect of BRCA1 in tumor cell lines. It was reported that overexpression of BRCA1 in human prostate (DU-145) and breast (MCA-7) cancer cells would protect cells against oxidative stress through enhancing NRF2 activity and stimulating ARE-driven transcriptional activity [10,11,31]. Besides, up-regulation of BRCA1 in these cancer cell lines reduces ROS production and protein nitration and also attenuates H_2O_2-induced oxidative DNA damage and apoptosis [10,11]. However, the role of BRCA1 in ischemic stroke remains unknown. In the present study, we found that overexpression of BRCA1 reduced ROS production and

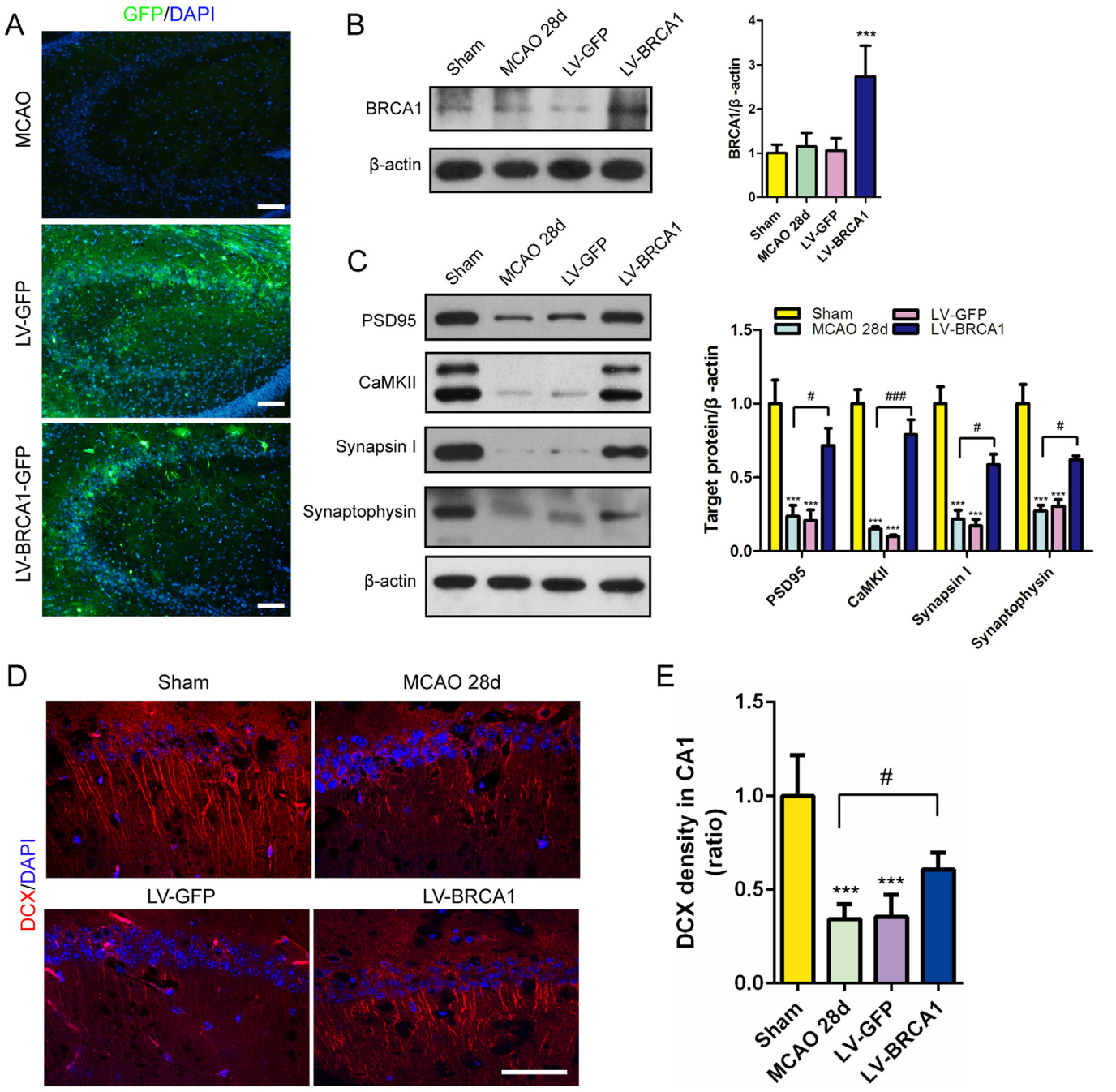

Fig. 8. LV-BRCA1 treatment facilitated synaptic plasticity after MCAO. (A, B) Transfection efficiency of LV-BRCA1 in hippocampus, n = 5. (C) Western blot and quantitative analysis of PSD95, CaMKII, Synapsin I and synaptophysin, n = 6. (D) Representative micrographs of DCX staining in CA1. (E) Quantification of DCX immunofluorescence density, n = 6. Scale bar = 50 μm. Data are expressed as mean ± SD; $^{***}P < 0.001$ versus sham group; $^{\#}P < 0.05$, $^{\#\#\#}P < 0.001$ versus MCAO group.

declined lipid peroxidation adducts, including MDA and 4-HNE, along with potentiated antioxidant enzyme SOD activity, resulting in attenuated cerebral oxidative damage. As a key component of endogenous antioxidant defense, NRF2 has been demonstrated to protect cerebral I/R injury [26]. In this study, we confirmed that NRF2 was a direct target of BRCA1 in ischemic brain. The overexpression of BRCA1 induced expression and nuclear translocation of NRF2, leading to the increase of ARE genes expression, including HO-1, NQO1 and GPX4 at transcriptional and post-transcriptional levels one day post ischemic stroke. Of these up-regulated genes, GPX4 is the only enzyme of GPXs family that can directly detoxify lipid hydroperoxides within cell membranes under various stresses, thereby reduce adduct products of lipid peroxidation and maintain membrane stability. Taking this into count, there are two items to explain the lipid peroxidation reduction in our study as following: i) as a subsequent consequence of decrement of ROS production; ii) directly reduced by GPX4.

It has been reported that BRCA1 interferes with conformational dynamics of NRF2-KEAP1 interaction at the ETGE motif of NRF2 to prevent NRF2 ubiquitin-dependent degradation [10]. However, the exact domain of BRCA1 with which NRF2 interacts has yet been exposed. BRCA1 contains two key functional domains, the amino terminal RING domain and the carboxyl terminal BRCA1 C-terminal (BRCT) motifs, both of which are of utmost importance for BRCA1 activity [8,32]. Our study identified the BRCT domain (aa 1591–1784) of

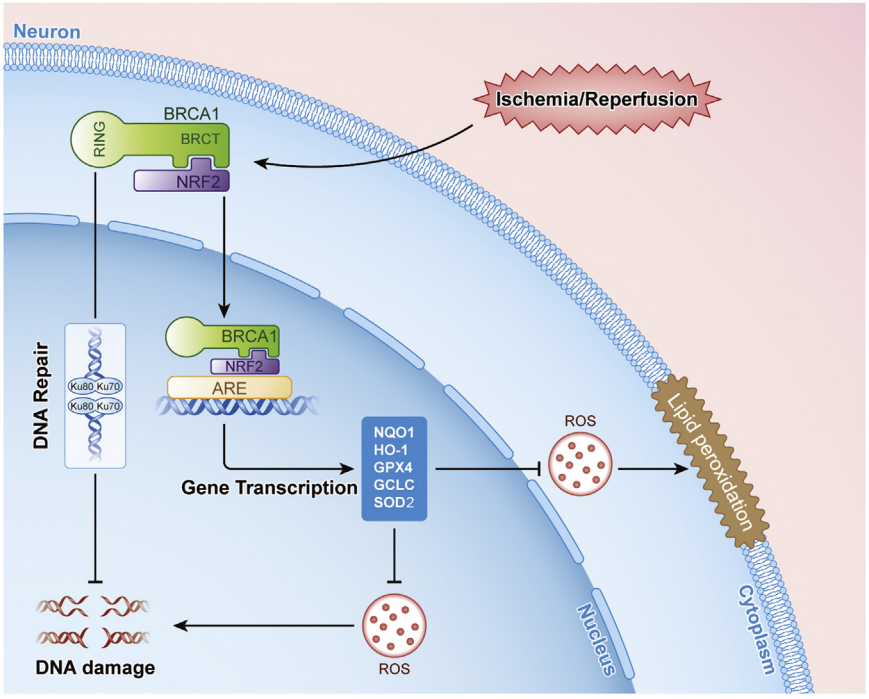

Fig. 9. Schematic depicting neuroprotective roles of BRCA1 towards I/R injury. Excessive ROS production damages macromolecule DNA and lipids. BRCA1 binds directly to NRF2 via its BRCT domain and facilitates NRF2-mediated antioxidant response. Then the downstream ARE genes, including HO-1, NQO1, GCLC, GPX4 and SOD2 are induced, which reduces ROS production and attenuates lipid peroxidation. Meanwhile, BRCA1 promotes DSBs repair through up-regulating Ku70/Ku80 in NHEJ pathway. As a result, neuronal cell death is inhibited.

BRCA1 as the specific domain to directly interact with NRF2 and activate the antioxidative NRF2/ARE signaling pathway. We also confirmed that BRCA1 binds to the XRE region of NRF2 promoter and regulates NRF2 transcription. However, another research group reported in conflict that transcription of BRCA1 is induced by NRF2 through the ARE site on BRCA1 promoter [33]. Accounting with the reports and our findings, there could be a positive feedback loop regulation between BRCA1 and NRF2, which monitoring the cellular antioxidation. In addition, previous studies have found that BRCA1 induces the expression of p21 which has been reported to directly interact with NRF2 and regulate the NRF2-mediated antioxidant response [34–36]. Therefore, it could be another pathway of BRCA1 to active NRF2 indirectly.

Oxidative DNA damage, a severe consequence of oxidative stress, happens in a variety of neurological disorders, including ischemic stroke, AD, Parkinson's disease and ALS [37–40]. The accumulation of DNA lesions, including base modifications, abasic sites, single and double strand breaks, can trigger neuronal cell death, if without effectively repair [41]. In AD, BRCA1 ablation in neurons was reported to cause the increase of DSBs, abnormal chromatin remodelling and cellular dysfunction [14], suggesting a critically role of BRCA1 in DSBs repair in CNS. However, the exact pathway through which BRCA1 repairs DSBs in neurons remains unclear. Accumulating studies have demonstrated that BRCA1 is involved in several DNA repair pathway, including HR repair, NHEJ repair, nucleotide excision repair (NER) and base excision repair (BER) pathway [8,24,40,42–44]. Among these repair pathways, BRCA1 is presumed to involve primarily in HR, which is not known to occur physiologically in non-dividing cells [40]. NHEJ, characterized by forming compatible ends through direct ligation, takes place in G0-, G1- and early S-phases of the cell cycle, which make it appears to be a critical DSBs repair mechanism in nondividing cells. Yet, a study examining myocardial infarction showed that BRCA1 contributes to RAD5-foci formation suggesting that BRCA1 may govern HR repair of DSBs in nondividing cardiomyocytes [15]. Another research reported that BRCA1 is recruited in response to DNA damage in nondividing neuronal cells [27]. Taken all the above in account, we focused on HR and NHEJ repair in the present study and demonstrated that BRCA1 promoted DSBs repair through NHEJ pathway in neurons under I/R condition as reflected by enhancing Ku70 and Ku80 expression, whereas displayed no effect on RAD51-mediated HR repair. Heterogeneous dimerization of Ku70 and Ku80 forms Ku protein, which binds to DNA double strand break ends and is required for the NHEJ pathway of DNA repair [45]. Whether NER or BER pathway is involved in BRCA1 mediated DNA repair in mature neurons remains to be explicated in the future.

In hAPP transgenic mice, reduction of neuronal BRCA1 in dentate gyrus impaired long-term synaptic plasticity, resulting in hippocampal-dependent spatial learning and memory deficit [14]. In the present study, overexpression of neuronal BRCA1 in hippocampus improved cognitive function post-stroke. To explore the underlying mechanism of improving cognitive function after LV-BRCA1 administration, we evaluated synaptic plasticity by detecting synaptogenesis proteins, including PSD95, CaMKII, Synaptophysin and Synapsin I, and found that overexpression of BRCA1 enhanced these factors expression. Recent findings suggest that BRCA1 have a positive effect on neurites and dendritic spines formation [14,27]. We speculate that enhancement of BRCA1 could potentially benefit dendritic spine formation. And we observed that BRCA1 overexpression increased dendritic spine density as reflected by increased DCX immunostaining density. According to reports, BRCA1 distributes in embryonic and adult neurogenic areas, especially proliferating neuronal precursor cells, and plays a critical role in neurogenesis and brain development [23,46–48]. Moreover, BRCA1 ablation inhibits neural precursor cells (NPCs) proliferation and neuronal differentiation [23]. In our recent studies with neural stem cells (NSCs), we found that overexpression of BRCA1 promoted NSCs survival and proliferation (not shown here).

Several issues should be further investigated following the present study. First, whether BRCA1 regulates proliferation and differentiation of NPCs in neurogenic niche located in the subgranular zone of hippocampus, which may also contribute to cognitive function repair, needs further investigation. Second, BRCA1 may exert neuroprotective effect in ischemic stroke through other mechanisms distinct from those explored in our studies, which need further experiments to clarify.

In conclusion, this study demonstrated that BRCA1 protected neurons against I/R injury post-stroke. The neuroprotective effect of BRCA1 was mediated by its ability to interact with NRF2, repair damaged DNA and rescue cognitive dysfunction. These findings may encourage future studies on BRCA1 both in ischemic stroke and other

oxidative stress related neurodegenerative disease.

Acknowledgments

This work was supported partly by National Natural Science Foundation of China (No. 81571143, 81701230, 81701180), Jiangsu Natural Science Foundation (No. BK20160607).

Conflict of interest

The authors declare no conflicts of interest regarding the publication of this article.

Author contributions

Gelin Xu and Xinfeng Liu designed the experiment. Pengfei Xu and Qian Liu performed most of the experiments and drafted the manuscript. Yi Xie, Xiaolei Shi, and Yunzi Li contributed to neuron OGD model generation and lentivirus transfection. Mengna Peng, Hongquan Guo, and Rui Sun performed the MCAO model. Juanji Li and Ye Hong collected and analyzed the data. All authors have read and approved the final manuscript.

Appendix A. Supporting information

Supplementary data associated with this article can be found in the online version at doi:10.1016/j.redox.2018.06.012.

References

[1] G.J. Hankey, Stroke, Lancet 389 (10069) (2017) 641–654, https://doi.org/10.1016/S0140-6736(16)30962-X.
[2] S. Manzanero, T. Santro, T.V. Arumugam, Neuronal oxidative stress in acute ischemic stroke: sources and contribution to cell injury, Neurochem. Int. 62 (5) (2013) 712–718, https://doi.org/10.1016/j.neuint.2012.11.009.
[3] C.L. Allen, U. Bayraktutan, Oxidative stress and its role in the pathogenesis of ischaemic stroke, Int J. Stroke 4 (6) (2009) 461–470, https://doi.org/10.1111/j.1747-4949.2009.00387.x.
[4] D. Radak, I. Resanovic, E.R. Isenovic, Link between oxidative stress and acute brain ischemia, Angiology 65 (8) (2014) 667–676, https://doi.org/10.1177/0003319713506516.
[5] C. Dominguez, P. Delgado, A. Vilches, P. Martin-Gallan, M. Ribo, E. Santamarina, C. Molina, N. Corbeto, V. Rodriguez-Sureda, A. Rosell, et al., Oxidative stress after thrombolysis-induced reperfusion in human stroke, Stroke 41 (4) (2010) 653–660, https://doi.org/10.1161/STROKEAHA.109.571935.
[6] I. Ciancarelli, D. De Amicis, C. Di Massimo, A. Carolei, M.G. Ciancarelli, Oxidative stress in post-acute ischemic stroke patients after intensive neurorehabilitation, Curr. Neurovasc. Res. 9 (4) (2012) 266–273.
[7] D. Paspalj, P. Nikic, M. Savic, D. Djuric, I. Simanic, V. Zivkovic, N. Jeremic, I. Srejovic, V. Jakovljevic, Redox status in acute ischemic stroke: correlation with clinical outcome, Mol. Cell. Biochem. 406 (1–2) (2015) 75–81, https://doi.org/10.1007/s11010-015-2425-z.
[8] C.M. Christou, K. Kyriacou, BRCA 1 and its network of interacting partners, Biology (Basel) 2 (1) (2013) 40–63, https://doi.org/10.3390/biology2010040.
[9] Y.W. Yi, H.J. Kang, I. Bae, BRCA1 and oxidative stress, Cancers (Basel) 6 (2) (2014) 771–795, https://doi.org/10.3390/cancers6020771.
[10] C. Gorrini, P.S. Baniasadi, I.S. Harris, J. Silvester, S. Inoue, B. Snow, P.A. Joshi, A. Wakeham, S.D. Molyneux, B. Martin, et al., BRCA1 interacts with NRF2 to regulate antioxidant signaling and cell survival, J. Exp. Med. 210 (8) (2013) 1529–1544, https://doi.org/10.1084/jem.20121337.
[11] T. Saha, J.K. Rih, E.M. Rosen, BRCA1 down-regulates cellular levels of reactive oxygen species, FEBS Lett. 583 (9) (2009) 1535–1543, https://doi.org/10.1016/j.febslet.2009.04.005.
[12] A. Uryga, K. Gray, M. Bennett, DNA damage and repair in vascular disease, Annu. Rev. Physiol. 78 (2016) 45–66, https://doi.org/10.1146/annurev-physiol-021115-105127.
[13] T.A. Evans, A.K. Raina, A. Delacourte, O. Aprelikova, H.G. Lee, X. Zhu, G. Perry, M.A. Smith, BRCA1 may modulate neuronal cell cycle re-entry in alzheimer disease, Int. J. Med. Sci. 4 (3) (2007) 140–145.
[14] E. Suberbielle, B. Djukic, M. Evans, D.H. Kim, P. Taneja, X. Wang, M. Finucane, J. Knox, K. Ho, N. Devidze, et al., DNA repair factor BRCA1 depletion occurs in Alzheimer brains and impairs cognitive function in mice, Nat. Commun. 6 (2015) 8897, https://doi.org/10.1038/ncomms9897.
[15] P.C. Shukla, K.K. Singh, A. Quan, M. Al-Omran, H. Teoh, F. Lovren, L. Cao, Rovira II, Y. Pan, C. Brezden-Masley, et al., BRCA1 is an essential regulator of heart function and survival following myocardial infarction, Nat. Commun. 2 (2011) 593, https://doi.org/10.1038/ncomms1601.
[16] Y.Y. Lu, Z.Z. Li, D.S. Jiang, L. Wang, Y. Zhang, K. Chen, X.F. Zhang, Y. Liu, G.C. Fan, Y. Chen, et al., TRAF1 is a critical regulator of cerebral ischaemia-reperfusion injury and neuronal death, Nat. Commun. 4 (2013) 2852, https://doi.org/10.1038/ncomms3852.
[17] J. Chen, C. Zhang, H. Jiang, Y. Li, L. Zhang, A. Robin, M. Katakowski, M. Lu, M. Chopp, Atorvastatin induction of VEGF and BDNF promotes brain plasticity after stroke in mice, J. Cereb. Blood Flow. Metab. 25 (2) (2005) 281–290.
[18] Y. Xie, W. Liu, X. Zhang, L. Wang, L. Xu, Y. Xiong, L. Yang, H. Sang, R. Ye, X. Liu, Human albumin improves long-term behavioral sequelae after subarachnoid hemorrhage through neurovascular remodeling, Crit. Care Med. 43 (10) (2015) e440–e449, https://doi.org/10.1097/CCM.0000000000001193.
[19] L. Yang, Y. Jiang, Z. Wen, X. Xu, X. Xu, J. Zhu, X. Xie, L. Xu, Y. Xie, X. Liu, et al., Over-expressed EGR1 may exaggerate ischemic injury after experimental stroke by decreasing bdnf expression, Neuroscience 290 (2015) 509–517, https://doi.org/10.1016/j.neuroscience.2015.01.020.
[20] P. Xu, Y. Xu, B. Hu, J. Wang, R. Pan, M. Murugan, L.J. Wu, Y. Tang, Extracellular ATP enhances radiation-induced brain injury through microglial activation and paracrine signaling via P2X7 receptor, Brain Behav. Immun. 50 (2015) 87–100, https://doi.org/10.1016/j.bbi.2015.06.020.
[21] L. Xu, L. Wang, Z. Wen, L. Wu, Y. Jiang, L. Yang, L. Xiao, Y. Xie, M. Ma, W. Zhu, et al., Caveolin-1 is a checkpoint regulator in hypoxia-induced astrocyte apoptosis via RAS/RAF/ERK pathway, Am. J. Physiol. Cell Physiol. 310 (11) (2016) C903–C910, https://doi.org/10.1152/ajpcell.00309.2015.
[22] H.J. Kang, Y.B. Hong, H.J. Kim, O.C. Rodriguez, R.G. Nath, E.M. Tilli, C. Albanese, F.L. Chung, S.H. Kwon, I. Bae, Detoxification: a novel function of BRCA1 in tumor suppression? Toxicol. Sci. 122 (1) (2011) 26–37, https://doi.org/10.1093/toxsci/kfr089.
[23] G.M. Pao, Q. Zhu, C.G. Perez-Garcia, S.J. Chou, H. Suh, F.H. Gage, D.D. O'Leary, I.M. Verma, Role of BRCA1 in brain development, Proc. Natl. Acad. Sci. USA 111 (13) (2014) E1240–E1248, https://doi.org/10.1073/pnas.1400783111.
[24] K.W. Caestecker, G.R. Van de Walle, The role of BRCA1 in DNA double-strand repair: past and present, Exp. Cell Res. 319 (5) (2013) 575–587, https://doi.org/10.1016/j.yexcr.2012.11.013.
[25] W.M. Bonner, C.E. Redon, J.S. Dickey, A.J. Nakamura, O.A. Sedelnikova, S. Solier, Y. Pommier, Gammah2ax and cancer, Nat. Rev. Cancer 8 (12) (2008) 957–967, https://doi.org/10.1038/nrc2523.
[26] R. Zhang, M. Xu, Y. Wang, F. Xie, G. Zhang, X. Qin, NRF2-a promising therapeutic target for defensing against oxidative stress in stroke, Mol. Neurobiol. 54 (8) (2017) 6006–6017, https://doi.org/10.1007/s12035-016-0111-0.
[27] T. Mano, K. Nagata, T. Nonaka, A. Tarutani, T. Imamura, T. Hashimoto, T. Bannai, K. Koshi-Mano, T. Tsuchida, R. Ohtomo, et al., Neuron-specific methylome analysis reveals epigenetic regulation and tau-related dysfunction of BRCA1 in Alzheimer's Disease, Proc. Natl. Acad. Sci. USA 114 (45) (2017) E9645–E9654, https://doi.org/10.1073/pnas.1707151114.
[28] D.J. Bernard-Gallon, M.P. De Latour, V. Sylvain, C. Vissac, B. Aunoble, J. Chassagne, Y.J. Bignon, BRCA1 and BRCA2 protein expression patterns in different tissues of murine origin, Int. J. Oncol. 18 (2) (2001) 271–280.
[29] A.R. Silva, A.C. Santos, J.M. Farfel, L.T. Grinberg, R.E. Ferretti, A.H. Campos, I.W. Cunha, M.D. Begnami, R.M. Rocha, D.M. Carraro, et al., Repair of oxidative DNA damage, cell-cycle regulation and neuronal death may influence the clinical manifestation of Alzheimer's Disease, PLoS One 9 (6) (2014) e99897, https://doi.org/10.1371/journal.pone.0099897.
[30] H.N. Noristani, J.C. Sabourin, Y.N. Gerber, M. Teigell, A. Sommacal, M. Vivanco, M. Weber, F.E. Perrin, BRCA1 is expressed in human microglia and is dysregulated in human and animal model of ALS, Mol. Neurodegener. 10 (2015) 34, https://doi.org/10.1186/s13024-015-0023-x.
[31] I. Bae, S. Fan, Q. Meng, J.K. Rih, H.J. Kim, H.J. Kang, J. Xu, I.D. Goldberg, A.K. Jaiswal, E.M. Rosen, BRCA1 induces antioxidant gene expression and resistance to oxidative stress, Cancer Res. 64 (21) (2004) 7893–7909.
[32] C.X. Deng, S.G. Brodie, Roles of BRCA1 and its interacting proteins, Bioessays 22 (8) (2000) 728–737.
[33] Q. Wang, J. Li, X. Yang, H. Sun, S. Gao, H. Zhu, J. Wu, W. Jin, NRF2 is associated with the regulation of basal transcription activity of the BRCA1 gene, Acta Biochim. Biophys. Sin. (Shanghai). 45 (3) (2013) 179–187, https://doi.org/10.1093/abbs/gmt001.
[34] K. Somasundaram, H. Zhang, Y.X. Zeng, Y. Houvras, Y. Peng, H. Zhang, G.S. Wu, J.D. Licht, B.L. Weber, W.S. El-Deiry, Arrest of the cell cycle by the tumour-suppressor BRCA1 requires the cdk-inhibitor p21WAF1/CiP1, Nature 389 (6647) (1997) 187–190.
[35] T. Ouchi, S.W. Lee, M. Ouchi, S.A. Aaronson, C.M. Horvath, Collaboration of signal transducer and activator of transcription 1 (STAT1) and BRCA1 in differential regulation of IFN-gamma target genes, Proc. Natl. Acad. Sci. USA 97 (10) (2000) 5208–5213.
[36] W. Chen, Z. Sun, X.J. Wang, T. Jiang, Z. Huang, D. Fang, D.D. Zhang, Direct interaction between NRF2 andp21(CiP1/WAF1) upregulates the NRF2-mediated antioxidant response, Mol. Cell 34 (6) (2009) 663–673, https://doi.org/10.1016/j.molcel.2009.04.029.
[37] C. Canugovi, M. Misiak, L.K. Ferrarelli, D.L. Croteau, V.A. Bohr, The role of DNA repair in brain related disease pathology, DNA Repair (Amst.). 12 (8) (2013) 578–587, https://doi.org/10.1016/j.dnarep.2013.04.010.
[38] D.K. Jeppesen, V.A. Bohr, T. Stevnsner, DNA repair deficiency in neurodegeneration, Prog. Neurobiol. 94 (2) (2011) 166–200, https://doi.org/10.1016/j.pneurobio.2011.04.013.
[39] P. Li, X. Hu, Y. Gan, Y. Gao, W. Liang, J. Chen, Mechanistic insight into DNA damage and repair in ischemic stroke: exploiting the base excision repair pathway as a

model of neuroprotection, Antioxid. Redox Signal. 14 (10) (2011) 1905–1918, https://doi.org/10.1089/ars.2010.3451.
[40] R. Madabhushi, L. Pan, L.H. Tsai, DNA damage and its links to neurodegeneration, Neuron 83 (2) (2014) 266–282, https://doi.org/10.1016/j.neuron.2014.06.034.
[41] H. Li, N. Liu, G.K. Rajendran, T.J. Gernon, J.K. Rockhill, J.L. Schwartz, Y. Gu, A role for endogenous and radiation-induced DNA double-strand breaks in p53-dependent apoptosis during cortical neurogenesis, Radiat. Res. 169 (5) (2008) 513–522, https://doi.org/10.1667/RR1230.1.
[42] E.M. Rosen, BRCA1 in the DNA damage response and at telomeres, Front Genet. 4 (2013) 85, https://doi.org/10.3389/fgene.2013.00085.
[43] M. Isono, A. Niimi, T. Oike, Y. Hagiwara, H. Sato, R. Sekine, Y. Yoshida, S.Y. Isobe, C. Obuse, R. Nishi, et al., BRCA1 directs the repair pathway to homologous recombination by promoting 53BP1 dephosphorylation, Cell Rep. 18 (2) (2017) 520–532, https://doi.org/10.1016/j.celrep.2016.12.042.
[44] T. Saha, J.K. Rih, R. Roy, R. Ballal, E.M. Rosen, Transcriptional regulation of the base excision repair pathway by BRCA1, J. Biol. Chem. 285 (25) (2010) 19092–19105, https://doi.org/10.1074/jbc.M110.104430.
[45] J.R. Walker, R.A. Corpina, J. Goldberg, Structure of the ku heterodimer bound to DNA and its implications for double-strand break repair, Nature 412 (6847) (2001) 607–614.
[46] J.N. Pulvers, W.B. Huttner, BRCA1 is required for embryonic development of the mouse cerebral cortex to normal size by preventing apoptosis of early neural progenitors, Development 136 (11) (2009) 1859–1868, https://doi.org/10.1242/dev.033498.
[47] L. Korhonen, K. Brannvall, Y. Skoglosa, D. Lindholm, Tumor suppressor gene BRCA-1 is expressed by embryonic and adult neural stem cells and involved in cell proliferation, J. Neurosci. Res. 71 (6) (2003) 769–776.
[48] L.C. Gowen, B.L. Johnson, A.M. Latour, K.K. Sulik, B.H. Koller, BRCA1 deficiency results in early embryonic lethality characterized by neuroepithelial abnormalities, Nat. Genet. 12 (2) (1996) 191–194.